Spring 2019

Determining the Key Residues for Capsule Production in the GBS CpsA Protein

Anna Struba

DETERMINING THE KEY RESIDUES FOR CAPSULE PRODUCTION IN THE GBS CpsA PROTEIN

by

Anna Struba

A Thesis Submitted in Partial Fulfillment
of the Requirements for a Degree with Honors
(Biochemistry and Molecular/Cellular Biology)

The Honors College

University of Maine

May 2019

Advisory Committee:

Melody N. Neely, Associate Professor of Molecular and Biomedical Sciences, Advisor
Melissa Maginnis, Assistant Professor of Molecular and Biomedical Sciences
Joshua Kelley, Assistant Professor of Molecular and Biomedical Sciences
Robert Wheeler, Associate Professor of Molecular and Biomedical Sciences
Melissa Ladenheim, Associate Dean, Honors College

ABSTRACT

Streptococcus agalactiae (GBS) is a common bacterium found commensally in the vaginal mucosa of healthy adults. GBS also causes severe infection in neonates, often leading to meningitis, which can cause lifelong health consequences including impaired hearing and seizures. Infection of newborns mainly arises from a colonized mother, either before birth through ascending infection or during labor. Ascending infection, where the bacteria travel to the fetus from the vaginal mucosa, is especially concerning as it can lead to loss of pregnancy or premature birth. The most common method of neonatal GBS disease prevention is antibiotic prophylaxis during delivery, though this method is lacking in safety and application. A promising alternative target for GBS virulence attenuation involves capsular polysaccharide (CPS), which protects GBS from immune recognition and clearance. CPS is regulated by CpsA, a multifunctional protein which is implicated in transcriptional activation, and ligation of CPS to the cell wall via the LytR domain. In this study, a CpsA mutant was created with two amino acid substitutions in the LytR domain which were predicted to decrease LytR functionality. We used microscopy to determine that this mutant induced a change in chain length, as well FL-vancomycin to show that this phenotypic change was not due to a change in cell envelope structure. We measured CPS levels with an ELISA to show that this mutant causes a reduction in CPS level. Finally, we analyzed virulence in zebrafish of bacteria expressing the mutant and found that virulence was increased in WT GBS with this mutant.

TABLE OF CONTENTS

INTRODUCTION

Streptococcus agalactiae (GBS) is a bacterium found commensally in the vaginal mucosa of healthy adults (1). While commensal in adults, GBS also causes severe systemic infection in neonates. Neonatal diseases caused by GBS can be either early onset (appearing less than 7 days after birth) or late onset (appearing past the first 7 days) (5). Both presentations of the disease can have major short-term and long-term dangers, often leading to sepsis and meningitis, which can cause lifelong health consequences including impaired hearing and seizures (2). Infection of newborns can arise from a colonized mother via ascending infection through the chorioamniotic membrane, or from birth in which the neonate comes in direct contact with the colonized vaginal tract (3). Infection can additionally come from other colonized women who may have contact with the neonate after birth. Ascending infection, in which the bacteria move through the choriodecidual membrane to infect the fetus, is especially concerning as it can lead to loss of pregnancy or premature birth (17).

Pregnant women are tested for GBS colonization at around 35 weeks of pregnancy, and intrapartum prophylactic antibiotics are given to the mother during birth to prevent early onset disease, but this does not prevent late onset disease (5). Additionally, while the prevalence of GBS neonatal disease has declined since the rise in antibiotic prophylactics, the World Health Organization (WHO) estimated the global prevalence in 2017 to be 410,000 neonatal infections with 150,000 deaths (20). A likely major contributor to this high prevalence is that at-home births are more common in low-income due to lack of access to hospital care, and thus a hospital-administered antibiotic treatment is not a viable

option. Additionally, antibiotic use on pregnant women or on any infected neonate can have lasting effects on the child's immune development as well as the mother's own microbiome (21). Further emphasizing this concern is the possibility of selecting for GBS populations which are resistant to antibiotics, which could lead to further health considerations (4). Following these downfalls of current treatment methods, alternative methods of preventative GBS therapeutics would be very valuable for prevention of this infection.

Possible targets for GBS attenuation might include targeting of cell envelope components such as bacterial capsule. Capsular polysaccharide (CPS) is necessary in GBS for protection against phagocytosis and other immune responses (5, 6). In zebrafish models of GBS systemic infection, capsule production directly correlates to successful systemic infection (7). In particular, systemic infection is drastically impacted by deletion of the *cpsA* gene, the first gene in the capsule operon. In one study, wild type GBS (WT) had almost 100% mortality in adult zebrafish after 7 days. Comparatively, a deletion strain lacking *cpsA* gene (Δ*cpsA*) had below 40% mortality even after 7 days within the same study (7). Deletion of *cpsA* in GBS leads to a significant reduction in capsule production, possibly explaining the observed drop in zebrafish mortality (7).

CpsA is a 484 amino acid multifunctional protein common to all serotypes of GBS (8, 9). CpsA belongs to protein family LCP (LytR-CpsA-Psr), which is a protein family associated with creation and maintenance of the cell envelope (10). CpsA has four functional regions, namely an intracellular DNA-binding region with 3 transmembrane domains, an extracellular accessory domain, and an extracellular LytR domain. The DNA binding region was shown to bind specifically to the capsule operon promoter to

upregulate, or activate, operon transcription (7). Episomal, or extra-chromosomal plasmid-based, expression of this intracellular region alone causes a significant increase in Δ*cpsA* capsule levels. Episomal expression of full CpsA protein has the same effect, and neither significantly influence the WT strain.

While this intracellular region has a more conclusive function, the extracellular domains are less well understood. Crystal structure of homologous *S. pneumoniae* Cps2A shows separate folding of the accessory domain and LytR domain, and a pyro-phosphorylated polyprenol phosphate lipid was found within the LytR domain of the crystal structure (10). This could indicate that the LytR domain is responsible for CPS attachment, as CPS attachment to the peptidoglycan is thought to involve a carrier lipid (10). Despite these predictions, narrowing down the exact functional mechanism of this region has been challenging. Episomal expression of CpsA truncated immediately before the LytR domain doesn't complement for capsule production in Δ*cpsA*, and additionally causes a major decrease in capsule production in the WT strain (7). Following these findings, this dominant-negative effect was also observed with expression of a region between the accessory domain and the LytR domain (11), implicating this linker region in capsule production as well.

In addition to these associations with capsule production and cell wall maintenance, CpsA also appears to have a role in the length of streptococcal chains. Streptococcal chain length is has been reported to correlate to better host immune evasion in other streptococci, possibly due to better evasion of complement recognition in the blood (22). Because of this, variations in chain length could contribute variations in virulence. Δ*cpsA* strains are known to have large variability in chain length ranging from 2 cells per chain to far over

10 cells per chain, compared to WT's normal 2-5 cells per chain (11). In addition to decreasing capsule levels in WT strains, episomal expression of LytR-truncated CpsA causes an increase in chain length in WT strains which is normally only observed in the full knockout strain Δ*cpsA*. It is unclear how this morphology connects to the role of CpsA in capsule production, or how the loss of the LytR domain contributes to it. One proposed explanation involves LytR as a regulator of cell wall degradation during cell division (7). This role would be consistent with the results of the truncation tests, where LytR-truncation leads to decreased separation of newly divided cells.

Additionally, in Cps2A crystal structure was found a lipid co-isolate, indicating some role in lipid binding (10). The lipid was bound to a group of negatively charged, hydrophobic amino acids within Cps2A which are conserved in all LCP proteins. Several of these amino acids bind the phosphate head group of the lipid, such as R374 (R378 in GBS CpsA), whilst others are thought to aid bond stabilization, such as Q378 (Q382 in GBS CpsA) (10).

Based on these previous studies, the LytR domain is predicted to have some enzymatic role in CPS attachment, as well as chain length, possibly involving lipid binding. In order to study this potential LytR function in GBS, a mutant CpsA protein was created containing two substitution mutations at amino acid residues R378 (polar) and Q382 (charged). Both residues were mutated to the nonpolar amino acid alanine; if these two amino acids are necessary for LytR function, this change from polar and charged residues to nonpolar residues should lead to decreased functionality. Because LytR function is thought to involve regulation of chain length and CPS attachment, expression of this constructed mutant would produce an abnormal long chain and low CPS level phenotype

in WT GBS. To test these changes, the mutant CpsA was expressed in Δ*cpsA* and WT GBS variants. Chain length was quantified manually, cell envelope integrity was measured with a fluorescent marker, and CPS level was measured via an ELISA. Finally, the effects of the mutation on strain virulence was measured in zebrafish to better determine how the LytR domain of CpsA contributes to systemic survival *in vivo*. In this study we confirm in part a role of LytR domain ligation of CPS to the cell wall through a mechanism of binding the phosphate group of carrier lipids. We also confirm that neither tested residue is responsible for the abnormal chain lengths observed in previous studies with LytR-truncations. Finally, the R378A/Q382A mutant CpsA resulted in only minor changes to virulence in zebrafish embryos, and further research is required to determine whether the age of fish or size of dose were limiting factors.

METHODS

Bacterial strains and culturing

Plasmids were constructed using TOP10 strain of *Escherichia coli* (Invitrogen). Transformed *E. coli* cells were grown aerobically in Luria-Bertani (LB) broth, or on LB plates each with 20 μg/mL chloramphenicol and 1.4% agar (Dot Scientific). Strains 515 WT and 515 Δ*cpsA* of *S. agalactiae* were grown anaerobically in Todd-Hewitt broth (Dot Scientific) with 0.2% yeast extract and 3 μg/mL chloramphenicol. Cultures were grown on LB/Cam20 or THYB/Cam3 plates with 1.4% agar.

CpsA-R378A/Q382A plasmid construction

GBS 515 genomic DNA was used as a template with two sets of primers (1740/1942 and 1941/1672) to create two fragments of 1142 bp and 387 bp, respectively. Fragments were combined into one sequence using PCR SOEing with primers 1740 and 1672, yielding a fragment of 1493bp. This fragment was purified using GeneJet Plasmid MidiPrep Kit (ThermoScientific) and cloned into pLZ12-rofA using *Pst*I and *Bam*HI restriction sites. The resultant plasmid was transformed into *E. coli* for amplification and purification and selected on LB-Cam20 (20 μg/mL) agar plates. Transformation was confirmed with PCR (primers 1740 and 1672), then the plasmid was isolated using Purelink HiPure Plasmid Filter DNA Purification Kit (Invitrogen). This was transformed into both 515 Δ*cpsA* and 515 WT strains of GBS, and positive transformants were selected by growth on THYB-Cam3 (3 μg/mL) agar plates. Transformation into GBS strains was also

confirmed using PCR (using primers 1672 and 292 for WT and primers 1740 and 1672 for Δ*cpsA*). The final amino acid mutant is shown in Supplementary Fig. 1.

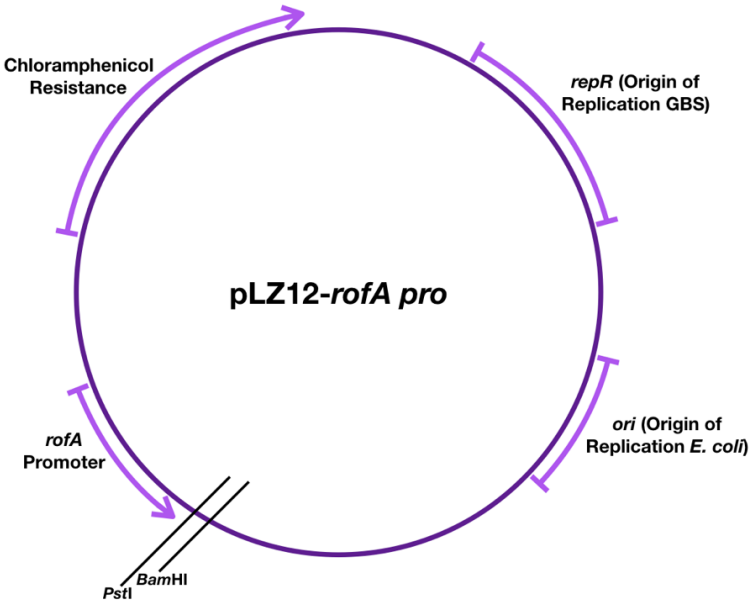

Figure 1. Plasmid map of the pLZ12-rofA-pro used to construct the final plasmid in this study. Vector DNA was stored in freezer stocks and isolated using a DNA isolation kit. The *Pst*I and *Bam*HI restriction sites were used as insertion sites for the mutant *cpsA*, and chloramphenicol was used as a selectable marker for positive *E. coli* and GBS transformants.

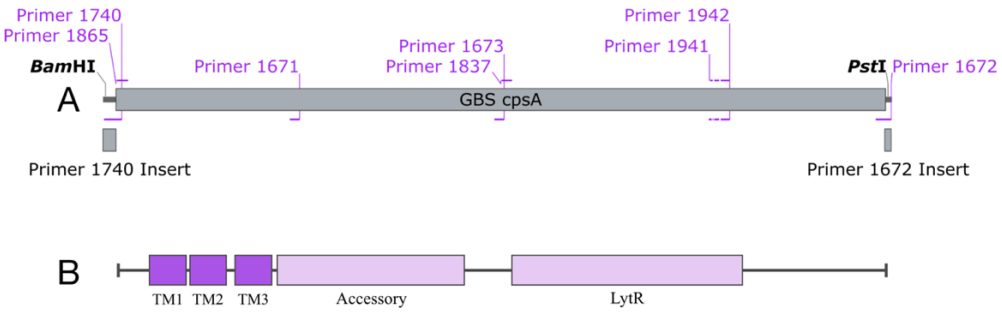

Figure 2. *cpsA* primer binding sites and mutation locations (A), and protein structural map (B). Mutation mapping was done using SnapGene (15), and structural mapping was adapted from UnitPro *cpsA* accession

Q9ALX6 (16). CpsA structure includes three transmembrane domains (TM), an accessory domain, and the LytR domain. GBS *cpsA* was isolated in two fragments using PCR; one primer from each primer set contained the desired double mutation. A full *cpsA* gene with the desired mutations was created from these fragments using a PCR SOEing reaction, and confirmed using gel electrophoresis. The final genomic fragment was digested with *Bam*HI and *Pst*I in preparation for ligation into the digested vector.

Table 1. Primers used for PCR and plasmid construction. Endonuclease cut sites are underlined.

Primer Name	*Abbreviation*	*5'– 3' Sequence*
5' GBS-CpsA-met	1865	ATGTCTAATCATTCGCGCCGTC
3' CpsA-del1-PstI	1671	GCTTCATACTCTGAAATTGAGTAACTGCAGTTTT
3' GBS CpsA-full-PstI	1672	GAACACAATGGAGGAATAACTGCAGTTTT
3' CpsA-LytR-Del-PstI	1673	CTTTTGGCTCTATATCAACATAACTGCAGTTTT
5' CpsA-Fwd-BglII	1837	TCAACAGTATCAAGATCTGATG
5' CpsA R378A/Q382A/Q3	1941	TAACGATGCAGGTAGAAATGCAGAAAAAGTGATTGCAGC
3' CpsA R378A/Q382A/Q3	1942	GCTAACGATGCAGGTAGAAATGCAGAAAAAAGTGATTGCAGC
5' GBS CpsA-RBS-BamHI	1740	GATTAGACATTGTAATTCTCCAATACGGATCCGCG
5'GFPuv-RBS-EcoRI	292	CCGGAATTCCGGAGGAGGAAAAATATGAGTAAAGGAGAAGAAC

FL-Vancomycin CpsA localization analysis

Δ*cpsA* and 515 strains of GBS were grown to an OD_{600} of 0.5 in ThyB-Cam3 broth. Cells were stained with BODIPY_FL vancomycin (Invitrogen) at 1μg/μL for 10 min, then transferred to a glass slides with coverslips. A Zeiss Axioscop fluorescence microscope was used for imaging.

Enzyme-linked immunosorbent assay (ELISA) capsule level analysis

Strains were grown in THYB-Cam3 broth grown at 37°C overnight. These cultures were normalized to OD_{600} of 0.75, pelleted, and washed 3 times with Tris-buffered saline + tween (TBST). Primary antibody (rabbit anti-Serotype 1a GBS) was diluted to 1:20,000, secondary antibody (secondary goat, anti-rabbit IgG conjugated to alkaline phosphatase (AP)) was diluted to 1:100. Secondary antibody was pre-adsorbed to prevent nonspecific binding using both Δ*cpsA* and WT GBS strains. Cells were incubated with 1μL primary antibody at 4˚C for 1 hr before 3 TBST washes. Cells were then incubated with secondary antibody for 1 hr at 4˚C before 3 TBST washes. Cells were resuspended in TBST and transferred to a 96-well plate. Alkaline phosphatase activity was measured after 1 hr dark incubation at 37°C after addition of p-nitrophenyl phosphate with alkaline phosphatase (Sigma). OD_{405} and OD_{600} were used to calculate activity, and each sample was done in triplicate.

Zebrafish virulence assays

Larval zebrafish infections were completed at 2 dpf using 2 nL injections into the yolk sac with 100 CFU inoculums of log phase bacterial cultures.

Statistical significance analyses

Numerical data was processed using a Student's T-Test, with Bonferroni and Holms post hoc.

RESULTS

In order to determine the functional amino acid residues of the LytR domain of CpsA, a CpsA-R378A/Q382A double mutant was created and expressed episomally in two GBS strains (Fig. 1, Fig. 2). Both amino acid residues are predicted to bind to the polar head group of the carrier lipid during CPS attachment. The effects of this mutation are therefore necessary to confirm this role. Previous reports demonstrated abnormal chain length and capsular phenotypes of the WT with *cpsA* truncations or deletions. Therefore, several methods were used to test these properties with the constructed mutant. Chain lengths were observed for Δ*cpsA* and WT strains using brightfield microscopy (Fig. 3, Fig. 4). Both strains expressing the vector (Δ*cpsA*-vector and WT-vector) were used as negative controls, and both strains expressing WT-CpsA (Δ*cpsA*-pWT-CpsA and WT-pWT-CpsA) were used as positive controls.

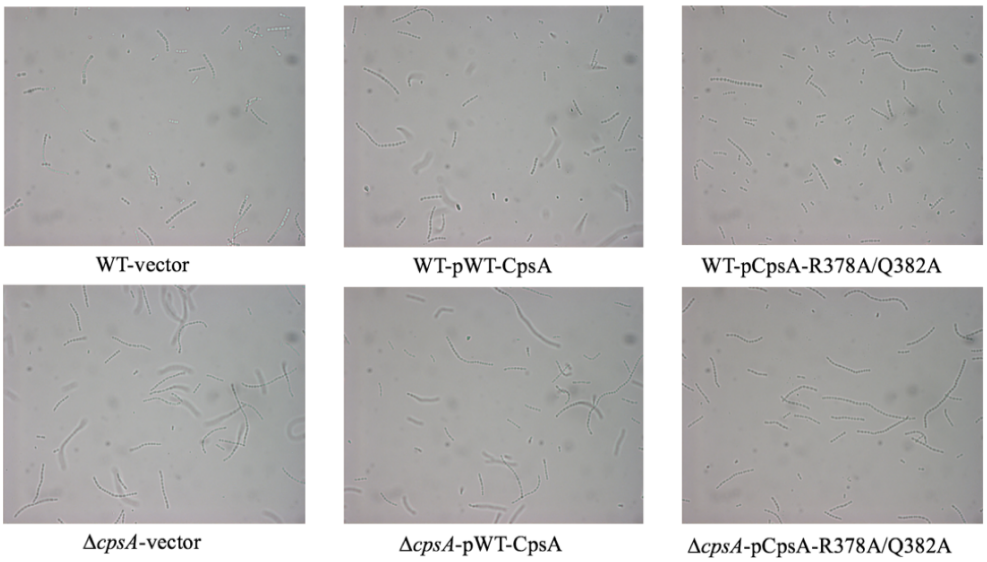

Figure 3. Chain length visualization with a brightfield microscope at 1000X magnification of Δ*cpsA* and WT

carrying the empty plasmid vector, the vector plus WT-CpsA, or the vector plus CpsA-R378A/Q382A as labeled.

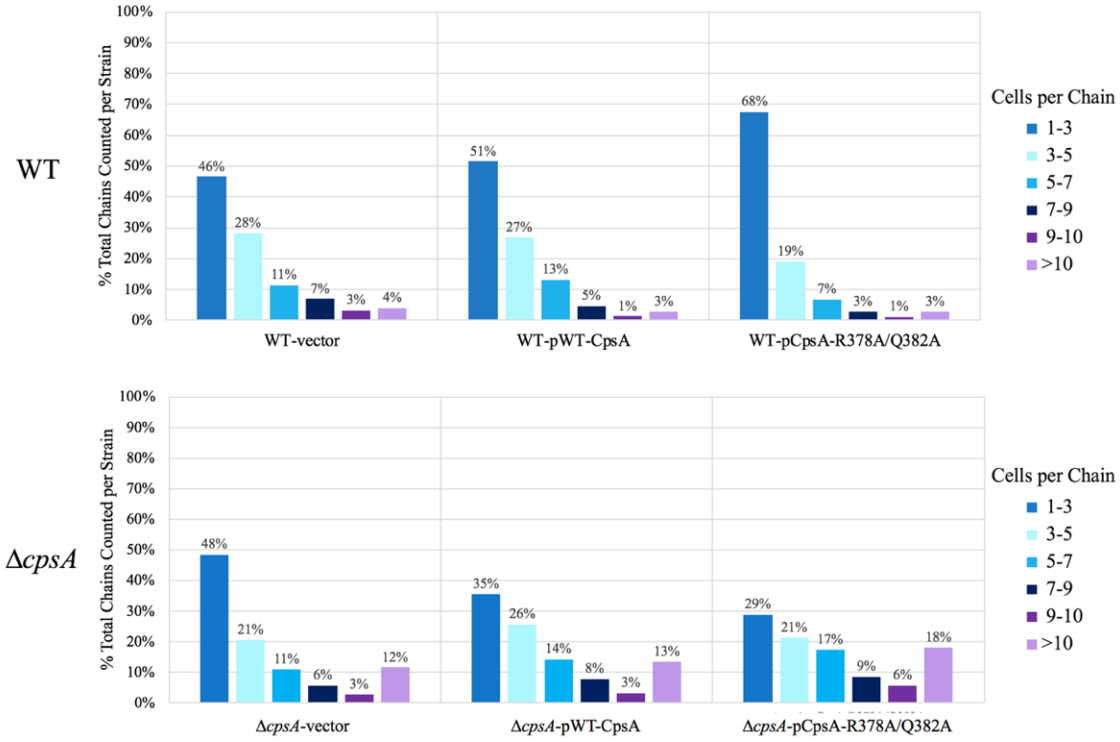

Figure 4. CpsA-R378A/Q382A induces an increase in short chain length in WT and does not complement for WT chain length in Δ*cpsA*. Chain length was quantified manually as the number of cells in each streptococcal chain using 20 brightfield non-overlapping microscopy images. Histograms were used to find the number of chains with 1–3, 3–5, 5–7, 7–9, 9–10, and >10 cells/chain for each sample, and frequency values were divided by the total number of chains to determine percentage of total chains in each length group.

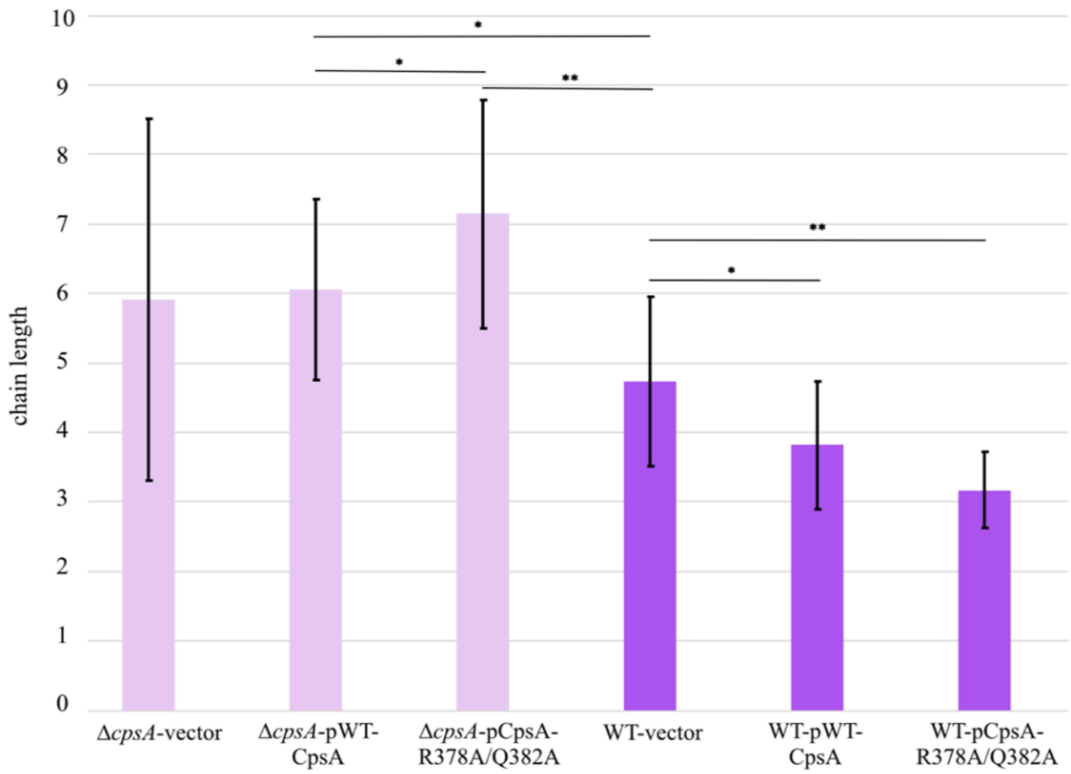

Figure 5. CpsA-R378A/Q382A induced an overall increase in average chain length in the Δ*cpsA* strain and a decrease in the average chain length in the WT strain. Chain length counts were averaged and measured for statistically significant change (*p<0.05, **p<<<<0.05). Error bars represent standard deviation.

Full LytR-truncated CpsA in previous studies has been shown to contribute to a long chain phenotype when expressed in WT GBS. We first questioned whether CpsA-R378A/Q382A would produce similar effects as this truncation, which would indicate that these residues are involved in this abnormal phenotype. Chain length has been shown to correlate to virulence, and thus any induced increase in chain length could indicate a decrease in virulence. Chain lengths were quantified manually from brightfield images (Fig. 3, Fig. 4). Both vector variants displayed a similar frequency of short chains less than 3 cells/chain; WT-vector strain had 46% while Δ*cpsA*-vector had 48% (Fig. 5). Both

variants had different long chains greater than 10 cells/chain; WT-vector had 4% while Δ*cpsA*-vector had 12%. Plasmid expression of WT-CpsA induced a slight decrease in frequency of longer chains in the WT, where chains of less than 3 cells/chain increased to 51%. In contrast, plasmid expression of WT-CpsA in Δ*cpsA* induced a decrease in the frequency of chains less than 3 cells/chain to 35% of the total chains counted. The WT-pCpsA-R378A/Q382A mutant had a much larger frequency of chains less than the WT-vector, with 68% of chains counted being shorter than 3 cells/chain. Δ*cpsA*-pCpsA-R378A/Q382A showed an overall decrease in short chain compared to Δ*cpsA*-vector, with 29% of chains having less than 3 cells/chain and 18% of chains having greater than 10 cells/chain.

In order to find statistically significant changes chain length in these strains, chain length averages were taken and compared using a T-test. The averages for each strain were 6 cells/chain (± 5 cells) and 5 cells/chain (± 2 cells), respectively. The chain length average for Δ*cpsA*-pWT-CpsA was 6 cells/chain (± 2 cells), while the WT-pWT-CpsA strain was 4 cells/chain (± 2 cells). The average for the Δ*cpsA*-pCpsA-R378A/Q382A strain was 7 cells/chain (± 3 cells), and the average for the WT-pCpsA-R378A/Q382A was 3 cells/chain (± 1 cells). There was a minor but significant increase in chain length in Δ*cpsA*-pCpsA-R378/Q382A compared to the Δ*cpsA*-vector and Δ*cpsA*-pWT-CpsA strains (7 cells/chain, 6 cells/chain, 6 cells/chain). Along with these changes in Δ*cpsA*, there was small significant decrease in chain length in the WT-pWT-CpsA compared to WT-vector (4 cells/chain, 5 cells/chain), and a large significant decrease in chain length in the WT-pCpsA-R378A/Q382A chain length (3 cells/chain). In comparing both strain variants, there was a significant increase in average chain length of the Δ*cpsA*-pCpsA-R378A/Q382A compared

to the WT-vector chain length (7 cells/chain, 5 cells/chain). A similar increase in average chain length was observed in the Δ*cpsA*-pWT-CpsA strain compared to WT-vector (6 cells/chain, 5 cells/chain). The connection between CpsA and these observed changes to chain length is unclear, but one potential explanation could involve the process of cell division. Streptococcal cell division involves partial degradation of the cell envelope connecting two cells, and thus CpsA could be involved somehow in regulating the frequency of this degradation.

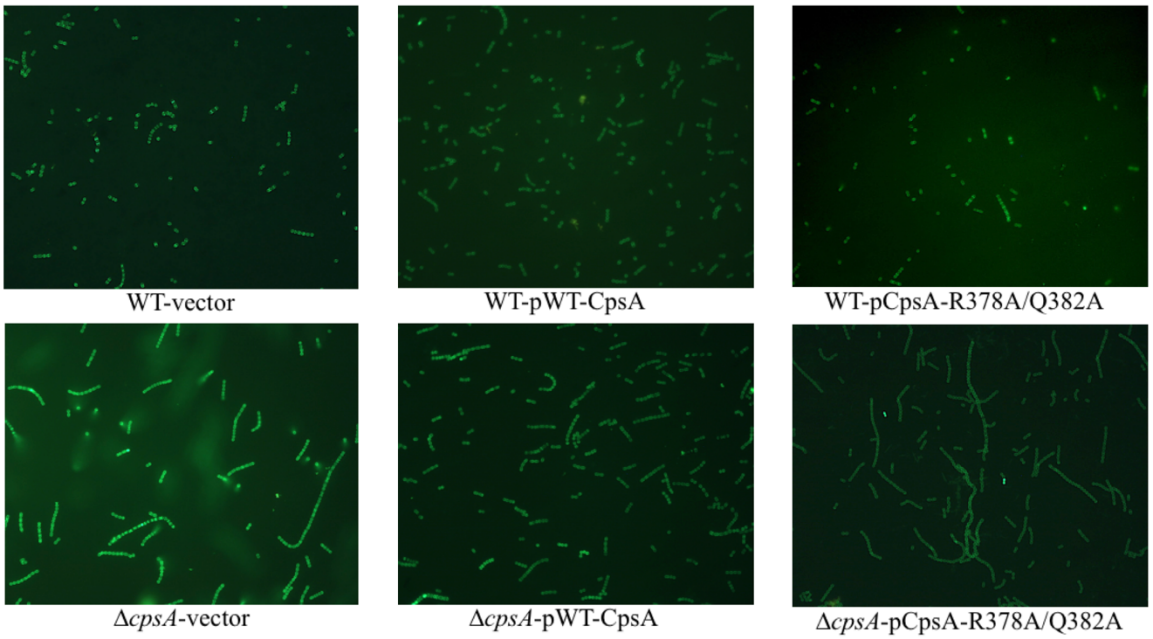

Figure 6. CpsA-R378A/Q382A does not induce a change in cell envelope morphology in WT or Δ*cpsA*. Cells were normalized to the same concentration, incubated with fluorescent vancomycin to visualize cell shape and peptidoglycan integrity, and viewed at 1000X magnification with a widefield fluorescent microscope.

Because the observed phenotypic changes in chain length could be due to a change in cell wall morphology, we questioned whether the cell wall shape had changed between

samples. Vancomycin is an antibiotic which binds to the peptidoglycan of bacterial cells, and therefore was used in conjugation with a fluorescent tag to more directly visualize the shape and integrity of the peptidoglycan layer (Fig. 6). Bacterial cells were stained with fluorescent vancomycin and viewed with a fluorescent microscope. No immediately noticeable abnormalities to cell symmetry, septal structure, nor cell viability were observed between samples. This indicated that the changes to chain length were likely not directly related to cell envelope structure.

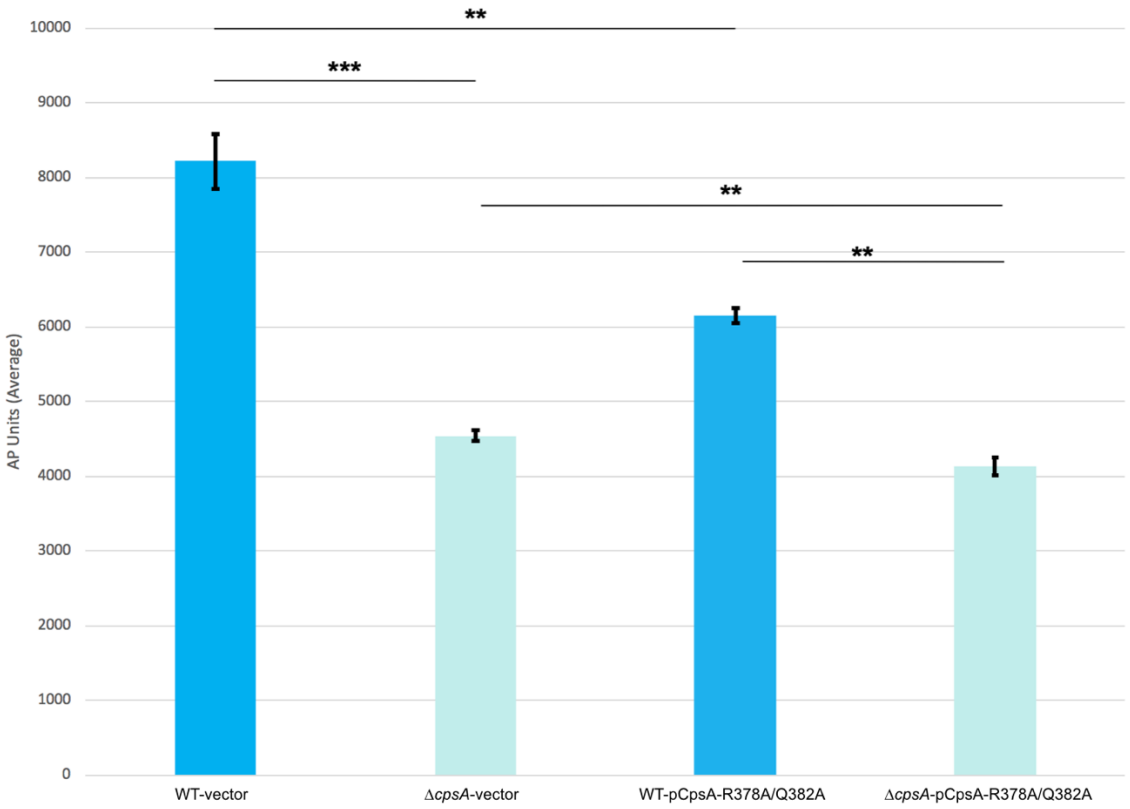

Figure 7. CpsA-R378A causes a dominant-negative decrease in CPS levels in WT strain and does not complement for CPS level in the Δ*cpsA* strain. An indirect ELISA was used to measure the levels of bound CPS for each strain variant. The secondary antibody was conjugated to alkaline phosphatase (AP), and AP

units therefore correlate to the level of membrane-bound CPS. Tests were done in triplicate for statistical analysis (**p<<0.05, ***p<<<<0.05, error bars represent standard deviation).

Following this abnormal chain length morphology, another major phenotypic change following expression of a full LytR-truncated CpsA from previous studies was a change in CPS level. Therefore, we next questioned whether CpsA-R378A/Q382A would produce this same effect, thus indicating that these residues are necessary for production or attachment of CPS. To measure CPS level, an indirect ELISA was performed using a primary antibody that binds to CPS. A secondary antibody which is conjugated to alkaline phosphatase binds to this primary antibody and converts the added PNPP substrate to the colored PNP, thus acting as an indicator level of bound secondary antibody. The level of CPS therefore directly correlates to alkaline phosphatase units (Fig. 7). Only the vector and CpsA-R378A/Q382A strain variants were utilized for this assay. Major significant decreases in capsule levels were observed between WT-vector and WT-pCpsA-R378A/Q382A (From around 8000 AP units to 6000 AP units), as well as between Δ*cpsA*-vector and Δ*cpsA*-pCpsA-R378A/Q382A (around 4500 AP units to 4000 units). Additionally, Δ*cpsA*-vector had significantly lower capsule levels compared to WT-vector (8000 AP units to 4500 units), and a similar result was noticed between both respective LytR-mutants (6000 AP units to 4000 units). Because CPS level is a necessary virulence factor for GBS, these reductions in CPS level could correlate to changes to the success and extent of systemic infection.

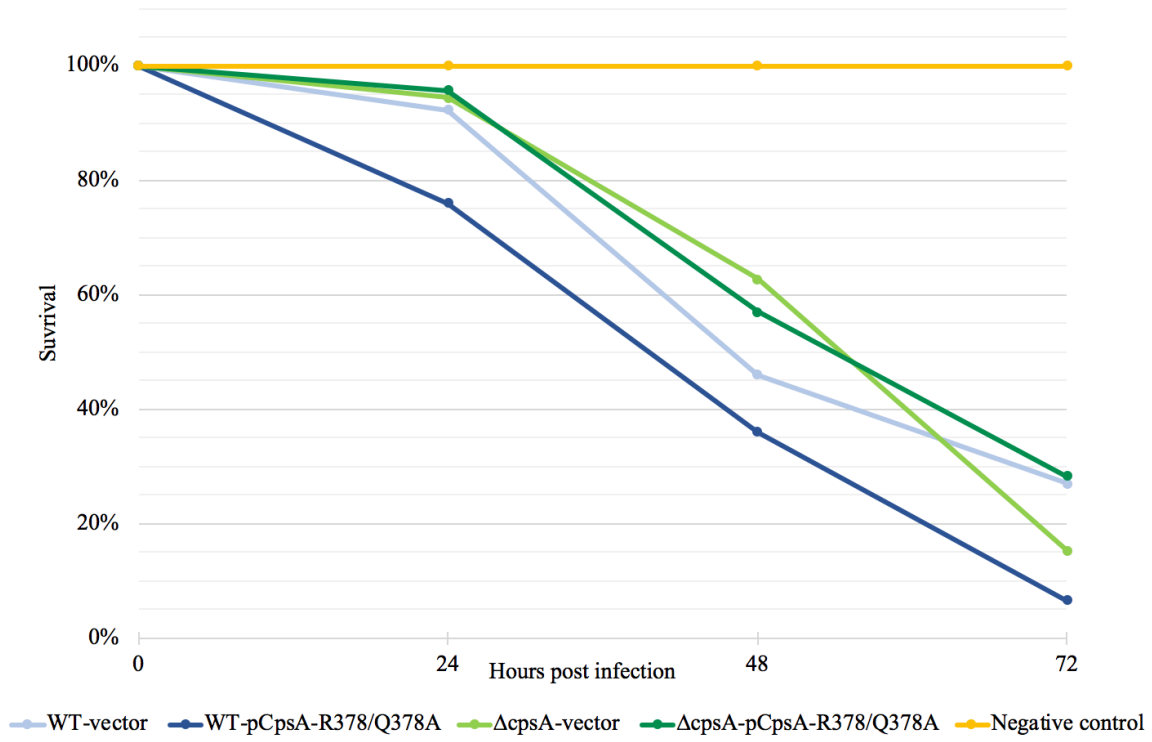

Figure 8. CpsA-R37A/Q382A caused WT GBS to be more virulent, and Δ*cpsA* to be less virulent. Survival curves were generated using 50 zebrafish larvae per sample at with 100 CFU yolk-sac infections. Zebrafish larvae were infected at 2 dpf and monitored every 24 hours for 72 hours.

Because increases in streptococcal chain length and reductions in CPS level have been associated with reductions in GBS virulence, the effects of CpsA-R378A/Q382A were observed *in vivo* with the zebrafish model. Zebrafish larvae were infected with the vector and mutant variants into the yolk sac and monitored for survival over 72 hours (Fig. 8). WT-vector, Δ*cpsA*-vector, and Δ*cpsA*-pCpsA-R378A/Q382A each had near 95% survival by 24 hours, while WT-pCpsA-R378A/Q382A had 76%. By 48 hours, Δ*cpsA*-vector had 63%, Δ*cpsA*-pCpsA-R378A/Q382Aa had 57%, WT-vector had 46%, and WT-pCpsA-R378A/Q382A had 36%. By 72 hours, both Δ*cpsA*-pCpsA-R378A/Q382A and WT-vector had near 30%, while Δ*cpsA*-vector had 15% and WT-pCpsA-R378A/Q382A

had 7%. Overall, WT-pCpsA-R378A/Q382A showed the highest increase in virulence compared to the vector variant, while Δ*cpsA*-pCpsA-R378A/Q382A showed the highest reduction in virulence compared to the vector variant.

DISCUSSION

GBS CpsA is a multifunctional regulator of cell envelope composition.

While GBS produces a variety of virulence factors, capsule is specifically crucial as it allows for survival in the host bloodstream by preventing destruction by immune factors. Capsule operon expression, CPS attachment, and cell wall maintenance are accomplished through interactions with the CpsA protein. The exact functional mechanism used by the CpsA protein is not well understood, but comparisons to homologous proteins have led to several intriguing predictions about particular domain function.

The LytR domain of GBS CpsA has homology to LytR proteins of other streptococcal bacteria such as *S. pneumoniae*. LytR proteins regulate capsule attachment and contribute to forming the septum, thus controlling cell size and chain length (12). When *S. pneumoniae* Cps2A is missing or nonfunctional, the LytR protein can complement for normal capsule production in place of CpsA (12). A strain of *S. pneumoniae* that suppressed both CpsA and LytR has a very abnormal phenotype which grows poorly and releases large amounts of CPS, indicating lack of capsule attachment (12). Crystal structure analysis of Cps2A also suggests a mechanism for this phenotypic change, in that the LytR domain of Cps2A binds lipids, consistent with a role in attachment of CPS to the cell wall (13).

Based on these data from studies on *S. pneumoniae,* the LytR domain of GBS CpsA was predicted to be associated with CPS attachment to peptidoglycan. In a previous study from our lab, mutations to the amino acids in the putative metal binding region of GBS CpsA expressed from a plasmid, prevented capsule production complementation in

the Δ*cpsA* strain, suggesting that the LytR domain uses metal ions to perform any respective functions (14). While this contributes to a confirmation for an enzymatic function of the LytR domain, little experimental evidence has been procured to confirm the exact role this function plays on chain length and capsule levels in GBS.

In order to address this gap in knowledge, a double mutant of CpsA was created with two polar to non-polar amino acid mutations in the LytR domain. The mutated amino acids residues, R378 and Q382, were predicted to bind to the phosphate head group of lipids based on Cps2A crystal structure data.

CpsA-R378A/Q382A causes reductions in long chain frequency in WT GBS.

To begin analysis of mutant CpsA, several strains of GBS with and without the constructed mutant were analyzed for chain length. The frequency variation for the deletion strain is lower than reported in previous studies, but Δ*cpsA* still had a higher proportion of chains greater than 10 cells/chain compared to WT. This is consistent with previous findings and suggest that deletion of CpsA contributes to increased chain length. The observed chain length trends indicate that the WT-CpsA does not complement for short WT chain length in ΔcpsA, but in fact increases it. Similarly, the CpsA-R378A/Q382A mutant induced an even greater reduction in short <3 cell chains, indicating that the mutant complements less than the WT-CpsA. Conversely, chain length frequency trends for the WT strain indicate that the LytR-mutant contributes to short chains being even more frequent.

Chain length averages for Δ*cpsA* had large variability, however, and therefore are unlikely to be meaningful despite slight statistical significance between the mutant and

pWT-CpsA variants. Conversely, WT-vector, WT-pWT-CpsA, and WT-pCpsA-R378A/Q382A show a significant downward trend in chain lengths, with the mutant having shorter average chain length than the WT-vector strain. Percentage graphs for the frequency of chain lengths additionally confirm this result, as chains with less than 3 cocci were much more frequent in the WT-pCpsA-R378A/Q382A strain compared to the WT-vector strain. Previous studies have indicated that expression of LytR-truncated CpsA in WT GBS causes a drastic change in chain length, with a majority of chains being longer than 10 cells (7). Because this long chain phenotype was not observed in the WT-pCpsA-R378A/Q382A variant, we can conclude that residues R378 and Q382 are not responsible for the long chain phenotype. Chain length quantification studies on additional LytR mutants would be necessary to determine the actual causative region of this phenotype. Such data would also provide a more expansive reference on the connection to chain length and CPS production; such connections cannot be made from the data herein. These data do suggest, however, that LytR-mutated CpsA causes WT chains become shorter. This could mean that the constructed mutation is gain-of-function for CpsA, or potentially that functional LytR domain interacts with cell wall degradation factors during cell division and thus non-functional LytR leads to aberrant regulation of chain length.

Cell wall FL-Vancomycin shows no visible changes in cell wall morphology.

Following chain length results, cell wall integrity was checked to determine if the mutant CpsA causes morphological abnormalities. No difference was noticed between any strain in terms of cell wall morphology after incubation with FL-vancomycin. Disruptions to cell wall morphology could indicate abnormal cell division or abnormal cell wall maintenance, which could be connected to predicted cell wall enzymes like LytR of CpsA.

However, because no abnormalities were observable here under brightfield microscopy, we cannot conclude that the CpsA-R378A/Q382A mutant affects cell wall maintenance. We can surmise, however, that residues R378 and Q382 are likely not major contributors to regulation of cell division or cell shape, as no aberrant septum formation or cell shape was noted.

CpsA-R378A/Q382A causes decreased CPS level in both Δ*cpsA* and WT GBS.

ELISA data confirmed previous findings that WT GBS has much higher CPS levels than the Δ*cpsA* strain, with a statistically significant difference of around 3600 AP units between the two strains. Interestingly, expression of CpsA-R378A/Q382A in both WT and Δ*cpsA* strains caused a significant decrease in CPS production from each respective control strain, thus indicating that the substitution mutations to the LytR domain do indeed cause a decrease in CPS production, or alternatively in CPS attachment, as any unbound-CPS was washed off of the cells before the assay. Quantification of CPS levels unbound to cells (*i.e.* supernatant from washes) would be necessary to determine which conclusion is more likely. Higher levels of CPS in the supernatant of the Δ*cpsA*-pCpsA-R378A/Q382A strains would likewise indicate that the observed decrease in bound capsule is in fact due to lack of attachment, rather than lack of CPS production or expression. Additionally, the decrease in CPS levels likely involves a repressive effect on WT CpsA because the downregulation of CPS levels was observed in a GBS strain which produces endogenous and fully-functional CpsA. Previous studies have suggested that the LytR domain acts as a ligase, transferring CPS from a carrier lipid to peptidoglycan via phosphate transfer reactions (13, Supplementary Fig. 2). Overall, we propose that the substitution mutation to the LytR

domain yields a non-functional or mis-functional protein which cannot attach CPS to the peptidoglycan as well as WT CpsA, and additionally impedes WT-CpsA function through some repressive, dominant negative effect.

CpsA-R378A/Q382A has a minor effect on virulence in zebrafish.

The zebrafish model is a proven model for neonatal systemic GBS infection (12). Larval zebrafish are especially useful as they have not yet developed an adaptive immune system and display an acute infection response that is easy to identify. On top of this, zebrafish embryos are transparent, meaning that live infection responses can be monitored visually through labeled innate immune factors. Research on CpsA has revealed that Δ*cpsA* caused significantly lower mortality in zebrafish than the WT model (12). Studies on bacterial burden in major zebrafish organs showed additionally that Δ*cpsA* has less dissemination in zebrafish than WT, and that CpsA truncated before the LytR domain had even further reductions in dissemination (11). Further, human whole blood analysis indicated that GBS with LytR-truncated CpsA had much lower survival than WT and Δ*cpsA* strains (12).

Previous studies noted major significant decrease in mortality between the Δ*cpsA* and WT variants of GBS (11,12). The results herein are not fully consistent with these findings, as WT-vector was only more virulent than Δ*cpsA*-vector at 48 hpi; Δ*cpsA*-vector was in fact more virulent than WT-vector at 72 hrs. WT-pCpsA-R378A/Q382A was the most virulent strain, with a consistent 10–20% mortality at each timepoint. These differences are minimal compared to the 60% difference observed in adult zebrafish in Rowe *et al* (11). It's possible that the LytR-mutant created a more virulent WT GBS strain, but it is more likely that these results were due to the experimental design. Because

previous studies reported GBS infection in adult zebrafish, it's possible that zebrafish embryos are not ideal for use of altered strains. The WT GBS variant is highly virulent likely as a result of excellent control of CPS levels, resulting in decreased levels for macrophage infection and transport to target tissues, as well as increased levels inside macrophages or during colonization to prevent immune cell-mediated degradation. The Δ*cpsA* strain as well as the R378A/Q382A variants, however, have large reductions in such CPS. Perhaps, recognition by immune cells is enhanced as a result to a higher degree than each phagocyte can handle, thus resulting in the infection spreading regardless throughout the bloodstream into every tissue. Further experiments would be necessary using lower doses to determine if the embryo model can be utilized for such experiments in the future. Alternatives could additionally include intramuscular injection of adult zebrafish which might be better suited to longer term survival monitoring.

CONCLUSIONS

These findings as a whole are consistent with the function of the LytR domain of CpsA as a catalyst for CPS attachment to the peptidoglycan. CPS attachment to peptidoglycan in streptococci is thought to involve polysaccharide synthesis, linkage of the CPS to lipid carriers, and transfer of CPS from the inside of the cell to the outside using phosphate transfer reactions (13, Supplementary Fig. 2). This transfer would involve CpsA acting as an enzyme catalyst, and this process has been experimentally confirmed to require a metal ion like Mg2+ (10, 16). The decreases in CPS levels induced by R378A/Q382A expression observed herein are consistent with such a mechanism, in that less CPS is ligated to the peptidoglycan because the residues responsible for carrier lipid binding no longer have the necessary negative charge. In addition to this finding, the CpsA-R378A/Q382A mutant did not cause an increased chain length phenotype when expressed in WT GBS, likely indicating that neither of these amino acid residues is responsible for the abnormal chain length phenotype observed in previous research. CpsA-R378A/Q382A caused WT GBS to be more virulent than the WT-vector strain, but additionally caused an decrease in virulence in Δ*cpsA*. Further experiments are necessary to fully confirm these results, as well as to determine their application to human therapeutics.

VI. FUTURE DIRECTIONS

This study confirmed in part the importance of residues R378 and Q382 of CpsA in production of CPS in GBS. Targeting of regions such as these could be very valuable, as CpsA-target vaccines for GBS would be non-serotype specific. These findings are not sufficient on their own to explain the full mechanism of CpsA function, as many amino acids are predicted to be involved in lipid binding. As such, each of these additional residues should also be analyzed for contributions to phenotypic changes in order to determine the full spectrum of activity of this protein. Analysis of supernatant from each mutant strain is also necessary to definitively confirm that the LytR domain mutations are responsible for decreased attachment, rather than decreased capsule operon transcription and CPS production. Finally, further zebrafish model analysis is necessary to better elucidate the effects of these CpsA mutations on virulence, and whether the dosage or age of the fish had an effect on the observed results.

REFERENCES

1. Carl MA, Ndao IM, Springman AC, Manning SD, Johnson JR, Johnston BD, Burnham CA, Weinstock ES, Weinstock GM, Wylie TN, Mitreva M, Abubucker S, Zhou Y, Stevens HJ, Hall-Moore C, Julian S, Shaikh N, Warner BB, Tarr PI. 2014. Sepsis from the gut: the enteric habitat of bacteria that cause late-onset neonatal bloodstream infections. Clin Infect Dis, 58:1211–1218.

2. Kim BJ, Hancock BM, Del Cid N, Bermudez A, Traver D, Doran KS. 2015. *Streptococcus agalactiae* infection in zebrafish larvae. Microb Pathog, 79: 57–60.

3. Maisey HC, Doran KS, Nizet V. 2008. Recent advances in understanding the molecular basis of group B Streptococcus virulence. Expert Rev Mol Med, 10:27.

4. Verani JR, McGee L, Schrag SJ. 2010. Prevention of perinatal group B streptococcal disease–revised guidelines from CDC, 2010. MMWR Recomm. Rep. 59:1–36.

5. Vornhagen J, Waldorf KA, Rajagopal L. 2017. Perinatal Group B Streptococcal Infections: Virulence Factors, Immunity, and Prevention Strategies. Trends in Microbiology, 25(11): 919-931.

6. Locke JB, Locke JB1, Colvin KM, Datta AK, Patel SK, Naidu NN, Neely MN, Nizet V, Buchanan JT. 2007. *Streptococcus iniae* capsule impairs phagocytic clearance and contributes to virulence in fish. J. Bacteriol, 189(4):1279-87.

7. Hanson BR, Runft DL, Streeter C, Kumar A, Carion TW, Neely MN (2012). Functional Analysis of the CpsA Protein of *Streptococcus agalactiae.* J. Bacteriol, 194(7):1668

8. Cieslewicz MJ, Kasper DL, Wang Y, Wessels MR. 2001. Functional analysis in type Ia group B Streptococcus of a cluster of genes involved in extracellular polysaccharide production by diverse species of streptococci. J Biol Chem 276:139-146.

9. Morona JK, Morona R, Paton JC. 2006. Attachment of capsular polysaccharide to the cell wall of *Streptococcus pneumoniae* type 2 is required for invasive disease. Proc Natl Acad Sci USA 103:8505.

10. Kawai Y, Marles-Wright J, Cleverley RM, Emmins R, Ishikawa S, Kuwano M, Heinz N, Bui NK, Hoyland CN, Ogasawara N, Lewis RJ, Vollmer W, Daniel RA, Errington J. 2011. A widespread family of bacterial cell wall assembly proteins. EMBO J 30:4931–4941.

11. Rowe HM, BR. Hanson, DL. Runft, Q. Lin, SM. Firestine, MN. Neely. 2015. Modification of the CpsA Protein Reveals a Role in Alteration of the *Streptococcus agalactiae* Cell Envelope. ASM, 83(4):1497-1506.

12. Hanson BR, Neely MN. 2011. Coordinate regulation of Gram-positive cell surface components. Current Opinion in Microbiology, 15:1–7.

13. Eberhardt A, Hoyland CN, Vollmer D, Bisle S, Cleverley RM, Johnsborg O, Håvarstein LS, Lewis RJ, Vollmer W. 2012. Attachment of Capsular Polysaccharide to the Cell Wall in *Streptococcus pneumoniae*. Mary Ann Liebert, 18:240-255.

14. SnapGene software (from GSL Biotech; available at snapgene.com).

15. Chen C, Huang H, Wu CH. Protein Bioinformatics Databases and Resources. 2017. Methods Mol. Biol. 1558:3-39. UniProtKB accession Q9ALX6.

16. M. N. Neely Lab, Unpublished data, 2018.

17. U.S. Department of Health & Human Services. Group B Strep (GBS). 2018. National Center for Immunization and Respiratory Diseases, Division of Bacterial Diseases. https://www.cdc.gov/groupbstrep

18. Gish, W. & States, D.J. (1993). Identification of protein coding regions by database similarity search. Nature Genet. 3:266-272.

19. Chatfield C., Koo H., and Quivey Jr R.G. 2005. The putative autolysin regulator LytR in *Streptococcus mutans* plays a role in cell division and is growth-phase regulated. Microbiology, 151:625-631.

20. World Health Organization. 2017. Group B Streptococcus Infection Causes an Estimated 150,000 Preventable Stillbirths and Infant Deaths Every Year. World Health Organization: Immunization, Vaccines, and Biologicals. www.who.int/immunization/newsroom/press/news_group_b_strep_stillbirths_infant_deaths_2017/en/.

21. Arboleya S., Sánchez B., Solís G., Fernández N., Suárez M., Hernández-Barranco A.M., Milani C., Margolles A., De los Reyes-Gavilán C.G., Ventura M., and Gueimonde M. Impact of Prematurity and Perinatal Antibiotics on the Developing Intestinal Microbiota: A Functional Inference Study. Int. J. Mol. Sci. 2016. 17(5):649.

APPENDIX: FUNDING AND SUPPLEMENTARY FIGURES

Funding: This work was made possible in part by the support of the Charlie Slavin Research Fund.

```
Query  1    MSNHSRRQQKKHSHTPLRVINLFLLVIFILLSVVSLFLMYRHHFLAFRHLNVIYGVVIVL  60
            MSNHSRRQQKKHSHTPLRVINLFLLVIFILLSVVSLFLMYRHHFLAFRHLNVIYGVVIVL
Sbjct  1    MSNHSRRQQKKHSHTPLRVINLFLLVIFILLSVVSLFLMYRHHFLAFRHLNVIYGVVIVL  60

Query  61   IILASLFLCIKNKARIFTTIILVLASIFVATTLYGFKSTIDLTNNLNKTASYSEIEMSVI  120
            IILASLFLCIKNKARIFTTIILVLASIFVATTLYGFKSTIDLTNNLNKTASYSEIEMSVI
Sbjct  61   IILASLFLCIKNKARIFTTIILVLASIFVATTLYGFKSTIDLTNNLNKTASYSEIEMSVI  120

Query  121  VPKDSKITNIEAVSKLAAPVKNDTSNITDLIEHIKSEKGISITPQKTDSYQDAYNRIKNG  180
            VPKDSKITNIEAVSKLAAPVKNDTSNITDLIEHIKSEKGISITPQKTDSYQDAYNRIKNG
Sbjct  121  VPKDSKITNIEAVSKLAAPVKNDTSNITDLIEHIKSEKGISITPQKTDSYQDAYNRIKNG  180

Query  181  DSQAMVLNNAYVSLIELSTPDFKSQIKTIYTYKIKKKINRKNTNHKEGVFNIYISGIDTF  240
            DSQAMVLNNAYVSLIELSTPDFKSQIKTIYTYKIKKKINRKNTNHKEGVFNIYISGIDTF
Sbjct  181  DSQAMVLNNAYVSLIELSTPDFKSQIKTIYTYKIKKKINRKNTNHKEGVFNIYISGIDTF  240

Query  241  GSISTVSRSDVNIIMTVNTNTHKVLLTTTPRDAYVKIPDGGGNQYDKLTHAGLYGVETSM  300
            GSISTVSRSDVNIIMTVNTNTHKVLLTTTPRDAYVKIPDGGGNQYDKLTHAGLYGVETSM
Sbjct  241  GSISTVSRSDVNIIMTVNTNTHKVLLTTTPRDAYVKIPDGGGNQYDKLTHAGLYGVETSM  300

Query  301  KTLENLYDINLDYYARINFSSFLKLIDLLGGVTVYNDQAFTSKHGNFDFPVGQVTLNSEQ  360
            KTLENLYDINLDYYARINFSSFLKLIDLLGGVTVYNDQAFTSKHGNFDFPVGQVTLNSEQ
Sbjct  301  KTLENLYDINLDYYARINFSSFLKLIDLLGGVTVYNDQAFTSKHGNFDFPVGQVTLNSEQ  360

Query  361  ALGFVRERYSLQGGDNDRGRNQEKVIAAIINKLASSQSVTKLNSITSQLQTSVQTNMTID  420
            ALGFVRERYSLQGGDND GRN EKVIAAIINKLASSQSVTKLNSITSQLQTSVQTNMTID
Sbjct  361  ALGFVRERYSLQGGDNDAGRNAEKVIAAIINKLASSQSVTKLNSITSQLQTSVQTNMTID  420

Query  421  NINDLINNQLSTGQRFTVESQALTGHGSTGELPSYAMPGAQLYMMSIDQSSLSNAKSKIK  480
            NINDLINNQLSTGQRFTVESQALTGHGSTGELPSYAMPGAQLYMMSIDQSSLSNAKSKIK
Sbjct  421  NINDLINNQLSTGQRFTVESQALTGHGSTGELPSYAMPGAQLYMMSIDQSSLSNAKSKIK  480

Query  481  NTMEE  485
            NTMEE
Sbjct  481  NTMEE  485
```

Supplementary Figure 1. WT CpsA (query) versus CpsA-R375A/Q382A (sbjct). The mutated region is indicated by upwards and downwards brackets. Alignment created using BlastP (18).

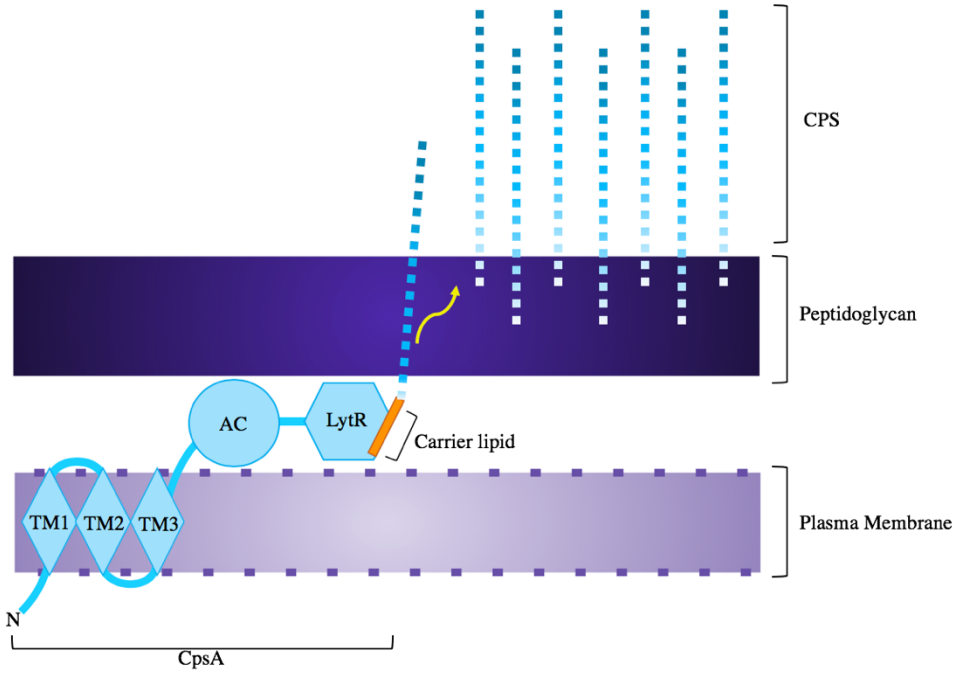

Supplementary Figure 2. Membrane topology and predicted function of CpsA. The LytR domain is predicted to bind carrier lipids for CPS and transfer the CPS to the peptidoglycan.

AUTHOR'S BIOGRAPHY

Anna is from Belfast, Maine and has lived in Maine her whole life. Anna is a Biochemistry major with a dual major in Molecular & Cellular Biology. She is passionate about insects and arachnids, and hopes to pursue a career in molecular biological research.